RESTORATION OF A LANDMARK BALANCED CANTILEVER BRIDGE CONSIDERING DIFFERENT RESILIENCE AND SUSTAINABILITY STRATEGIES

COMPDYN 2023
9th ECCOMAS Thematic Conference on
Computational Methods in Structural Dynamics and Earthquake Engineering
M. Papadrakakis, M. Fragiadakis (eds.)
Athens, Greece, 12-14 June 2023

# RESTORATION OF A LANDMARK BALANCED CANTILEVER BRIDGE CONSIDERING DIFFERENT RESILIENCE AND SUSTAINABILITY STRATEGIES

**Marco Domaneschi[1], Stergios A. Mitoulis[2], Raffaele Cucuzza[1], Valentina Villa[1] and Roberta Di Bari[3], Gopika Siva[2]**

[1]Politecnico di Torino, Department of Structural, Geotechnical and Building Engineering (DISEG), Corso Duca degli Abruzzi, Turin, Italy; e-mail: {marco.domaneschi, valentina.villa, raffaele cucuzza, giuseppe.marano} @polito.it

[2] Department of Civil Engineering, School of Engineering, University of Birmingham and www.infrastructuResilience.com; email: {S.A.Mitoulis, gxs268 } @Bham.ac.uk

[3] Department Life Cycle Engineering (GaBi), School of Engineering, Instute for Acoustics and Building Physics, Germany; email: roberta.di.bari@ibp.fraunhofer.de

**Abstract**

*This paper examines a landmark bridge upon which the road network functionality and life of people living in the region are heavily dependent. The Servia High Bridge, also known as the Lake Polyfytos Bridge, and it is the second longest bridge in Greece, spanning 1,372 meters. It was constructed by XEKTE SA and designed by Prof Riccardo Morandi. The bridge was designed around about the same time with the artificial Polyfytos lake, its construction started in 1972 and was completed in 1975. Strong connections exist between the nation's 48-year-old iconic bridge and the most significant power plants in South East Europe. The risk and resilience of the bridge and surrounding network have been assessed using a combination of visual inspections and digital data collection based on: (a) a digital twin, which provides a snapshot of the asset's current geometry and a dynamically evolving model that can inform advanced simulations; (b) satellite imagery, which offers ongoing updates and information about the asset's deformations and geometry; and (c) advanced numerical modeling, where based on back analysis an interpretation of the current deflections is attempted. The bridge exhibits degradation typically met in reinforced concrete (RC) and PRC (prestressed RC) bridges. In particular, the present case study is faced with challenges relating to the corroded tendons and concrete bonding. In this paper, different retrofitting measures are examined either the speed of recovery and the CO2 of the materials for retrofit, which reflect the resilience and sustainability of the examined strategies, based on FEM and monitoring data that lead to decisions.*

**Keywords:** bridge, sustainability, resilience, cost-effectiveness.

## 1 INTRODUCTION

Over the last 50 years, the balanced cantilever construction method has become prominent in bridge construction as it has proved itself to be both structurally effective and economically sound as a solution for medium spans, approximately 100 to 200 meters [1]. However, it is now evident that long-term effects of materials, such as creep and shrinkage of concrete and corrosion and relaxation of steel tendons, can cause damage to the deck, in the form of excessive vertical deflections of the cantilever ends an effect that was reported since the 90's by prominent researchers [2-4]. Numerous cases of bridge deterioration leading to excessive deflections have been documented before [5] with the damage in some instances extending to more than serviceability issues, e.g. resulting to partial collapse of the structure and fatalities. Although the main causes are almost positively confirmed to be the long-term effects, the ever-increasing traffic loads [6] and potential constructability issues [7], the detailed mechanism of the faults, as well as a streamlined method to calculate and predict them in a satisfactory level, are not yet established despite multiple researchers' endeavors [8-10].

The lack of a standard approach to this problem gave motivation to the authors to put forward an alternative solution, quite different approaches to the traditional ones that consist of multiple on-site inspections and measurements. This paper can be used in cases where the fragile nature of the asset and the uncertainty revolving its structural integrity poses as a barrier to destructive testing (e.g. loading with heavy vehicle) and extensive sample collection (e.g. cores of the deck concrete). In addition to that, as the construction sector is slowly but steadily moving towards digitalization and extensive monitoring, the proposed solution relies heavily on computer analysis and cutting-edge measuring tools such as drone-based photogrammetry [11], providing an inexpensive and time-efficient solution, while also being in accordance with environmental concerns. Laser scanning technology is rising in popularity [12] and has been found to achieve highly detailed results, even in restricted periods of time [13].

In this paper, a proposal using state-of-the-art surveying tools (laser-photogrammetry) paired with an advanced analysis is implemented to the Polyfytos bridge, a balanced cantilever segmentally constructed box girder bridge that developed excessive deformations and is now under investigation by the local Government and owner in Western Macedonia in Greece. The process begins with collecting data that were quite fragmented and scattered through the initial design report (written in 1974) and using it to create a 3D non-linear model of a typical cantilever (advanced modelling). After a thorough literature review, the most commonly mentioned possible causes of the problem were decided and a scenario based on each one was created (scenario-based modelling). The detailed measurements were compared to the results of the analyses and the scenarios were rated based on their resemblance to the actual state of the bridge.

The combination of the laser-scanning output and the detailed modelling deflection curves may be considered as evidence that can drive the project engineers to make a more precise assumption about the structural defects of the balanced cantilever part of the deck. Numerous examples across literature show that a misconception of the fault source may lead to erroneous repair methods, resulting in more extensive damage and sometimes even partial collapse [14]. At the same time, our proposal is time and cost efficient, carries little to no carbon footprint and helps engineers make decisions while having no physical interaction with the bridge.

### Background of the challenge

According to SGS [15], a leading inspection and verification multinational company, the usual process in damage assessment at an infrastructure asset includes a preliminary report, design supervision, on-site inspections, materials and construction units testing, monitoring and a final report of the repair process. However, there may be cases where one or more steps of this process are not feasible, and an alternative route should be followed in order to assess the condition of the asset. A technically sound solution to this problem should be in line with the two main contemporary principles around which all engineering innovation revolves nowadays; digitalization and sustainability.

The Polyfytos bridge is an asset built in 1975 in the Municipality of Western Macedonia, Kozani, Greece and bridges the artificial homonymous lake of Polyfytos, with the local and the national road network relying entirely on its integrity. The balanced cantilever method was used to build a part of the bridge, specifically six cantilevers spanning from piers 22, 23 and 24 (Fig.1) accounting for a total of 260 meters (total length of the bridge is 1372 m).

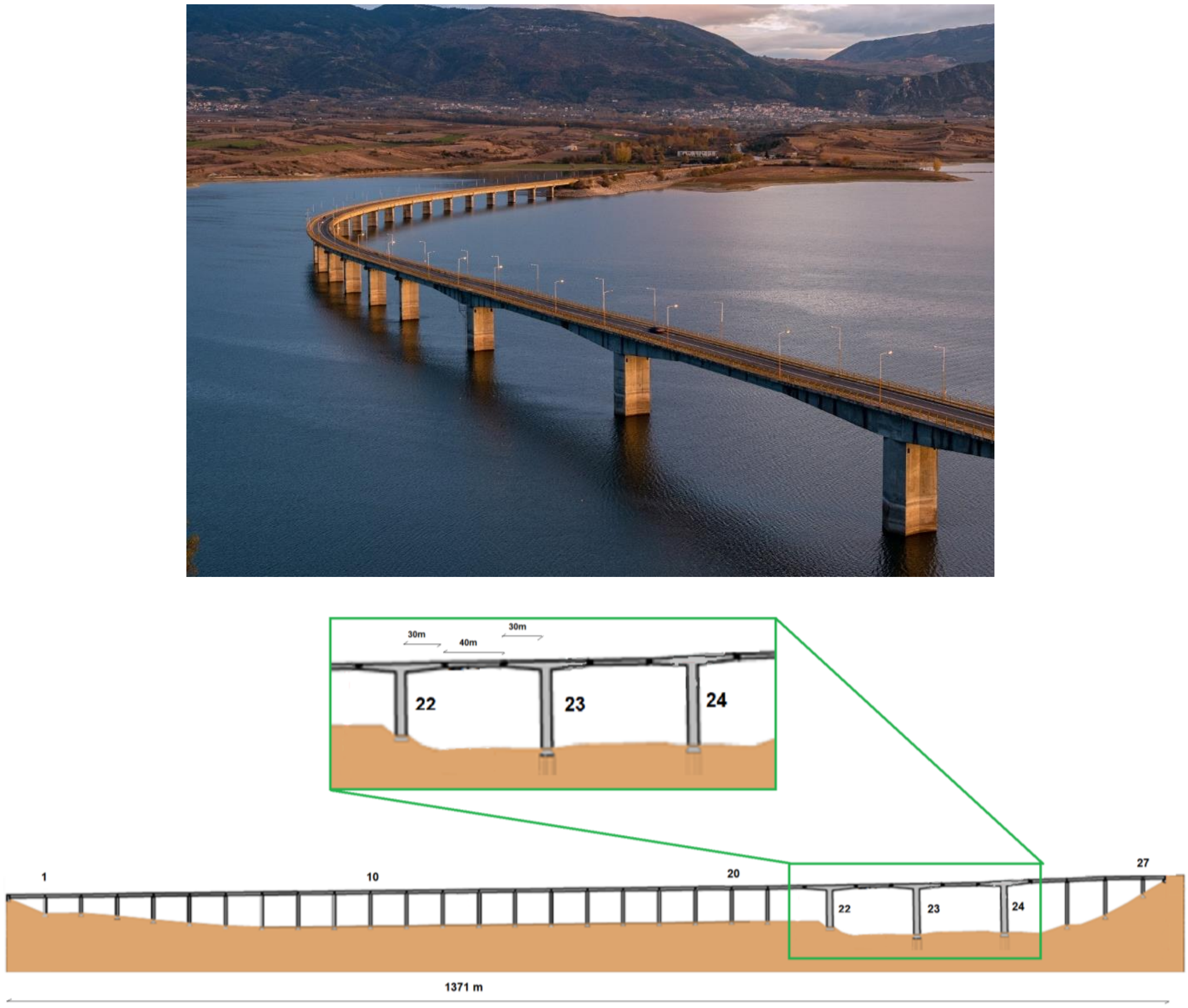


Figure 1: Bridge layout.

Very recently, excessive deflections at the free ends of the cantilevers were reported [16] during multiple inspections from inspectors and from one of the authors of this paper, a very common problem typically observed on old balanced cantilever bridges. Preliminary reports found evidence of corrosion and local concrete crashing, leading engineers to question the capacity and structural integrity of the bridge and as a result traffic restrictions were imposed, i.e. weight restrictions for heavy vehicles and reduction of the speed limit to minimize dynamic amplification impacts. The traditional way to extract meaningful conclusions about the condition of the materials would be extensive sampling, destructive testing methods and extensive vibration/loading checks, methods that was not authorized by the owners, as there are serious concerns about the bearing capacity of the deck at critical positions. At the same time, the road served by the bridge is part of a busy national road network traffic (part of the E65 Central Greece Highway) and detouring through the local road network is extremely difficult, and long, posing an extra challenge to engineers that would normally stop vehicles from crossing in order to conduct tests.

As a way to bypass many of the above-mentioned considerations our team proposes a digitalized approach to damage assessment, which can be applied on a wide range of structural assets (both residential and infrastructure) and relies heavily on state-of-the-art computational tools. Numerous approaches with different levels of interaction with the structure have been proposed through recent years, for example deflection-based monitoring system using sensor and signal processing technology [17] or connected pipe systems [18]. However, no approach is currently streamlined and considered as most optimum due to the fluctuating accuracy levels between the techniques in various occasions. The approach herein proposed as innovative contribution in the field requires minimum invasion and interaction with the structure, is extremely time efficient and includes minimal cost and carbon footprint.

The procedure starts with the fault report, where a decision has to be made around the degree on which on-site inspection and testing is allowed. In cases where the fragile nature of the structure poses as an obstruction, then high-tech surveying tools may be deployed. These tools should provide the engineers with viable information considering possible deflections, rotations, out-of-plane motions and even places where cracking is highly visible, all without ever setting foot on the actual structure. Two major options in order to obtain these measurements are drone-based photogrammetry (digital twin) and satellite imaging, with the former being chosen in the application of our proposal. Then the results should be interpreted and deflection curves should be created in order to provide a more mathematical view on the measurements, making them easier to compare with other data sets. At this point, any available information from official design reports should be also collected, however there might be cases where due to the passing of time they may have been misplaced or destroyed.

Based on design reports, information found in literature and scientifically backed assumptions, an advanced model of the structure is created. Contrary to the technological and academic advancements, numerous commonly found problems are not fully understood, leading to knowledge gaps that can only be approached in indirect ways. For example, the fault mechanism behind excessive deflections usually reported in balanced cantilever structures is not 100% documented yet, although creep and shrinkage have been observed by multiple research papers to play a significant part [19-22]. In order to save time, simplifications of some effects may be used when proven by literature to not significantly compromise result accuracy. The proposed way to cover multiple probable causes is a scenario-based analysis where each one will examine an individual parameter and its effect on the structure. In cases where the girder's behavior doesn't extend beyond its elastic limits, a simple superimposition is enough to examine the combined action of two or more parameters, although this is not possible in a non-linear analysis. Deflection curves from each scenario will be created in order to compare them with the measured results and conclude whether there is a data set that significantly resembles the initial ones in magnitude and/or shape.

If such a scenario is found, then engineers may use this approach as evidence to drive any possible investigation processes towards the probable cause that was used to create it. It should be clear that this method is not sufficient to produce absolute conclusions, it is a reliable source of information that may benefit both the engineers and the asset. Our proposal presents a highly digitalized, cost and time efficient solution, while also being environmentally friendly and requiring minimum interaction with the structure.

## A few words about corrosion

Corrosion in the tendons of prestressed concrete bridges is deemed to be among those principal factors that could undermine their structural integrity. Tendon corrosion failures/incidents have been reported in the past, e.g. the 1985 catastrophic failure of the prestressed Ynys-y-Gwas bridge in the United Kingdom that was constructed in 1953 without any prior warning [23], even at the early years in a bridge’s lifespan. For instance, several post-tensioned tendons were replaced in the Mid-Bay bridge in Florida due to corrosion related concerns only after eight years of its operation [24].

Herein, corrosion was assumed to be the main source of deterioration for the investigated bridge essentially disregarding additional failure mechanisms that might contribute (e.g. scouring, spalling of the reinforced concrete). In fact, when a strand is exposed to moisture its exposed interface becomes particularly prone to corrosion induced damages. Of particular concern is the so-called “localized corrosion” that could lead to substantial local reductions in the cross section of the stand and consequently to severe reductions of its tension capacity. Each strut could have (a) corroded and uncorroded wires within the same section and (b) corroded and uncorroded parts across its length.

## 2 BRIDGE DESCRIPTION

Located in the North-West part of the country, the Polyfytos bridge held the record for the largest overall length in Greece at the time of its construction, only surpassed by the Rio-Antirrio bridge almost 35 years later. The part of the bridge under interrogation consists of 3 segmentally constructed balanced cantilever sets, extending 30 meters either side of the abutments. Neighbouring cantilevers are connected by 40m long precast members forming an overall span of 100m (Fig. 1). The geometry and individual sizes of the segments were measured in the original drawings and verified on a point cloud model (Fig. 2).

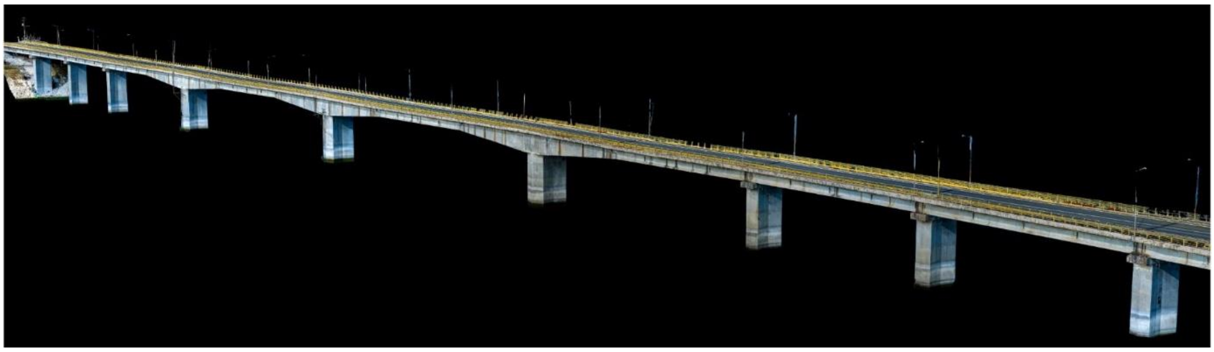

Figure 1: Point cloud model.

Prestressing concrete technique has been used in both the cantilever and precast beams (Fig. 3). The current view of the bridge deck with the original configuration of the prestressing cables in the cantilever beams and the precast beams between the half-joints is also depicted in Figure 3. Besides, Figure 4 reports the scheme of the current configuration of the bridge after about 50 years of in-service conditions. It can be seen that the failures of the brackets due to long-term material effects and the progression of prestressing cables in particular induced differential failures of the central beam between the half-joints. However, due to the property of the simply supported central beam, no additional coercive stresses developed.

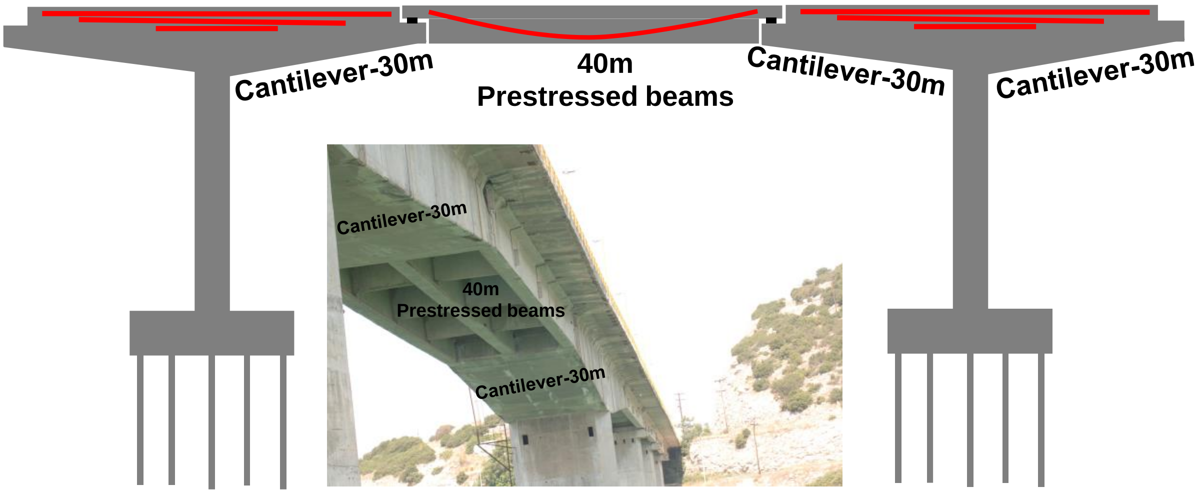


Figure 3: Schematic (not true) configuration with prestressing cables (red lines) and the actual view of the deck between Piers 23-24.

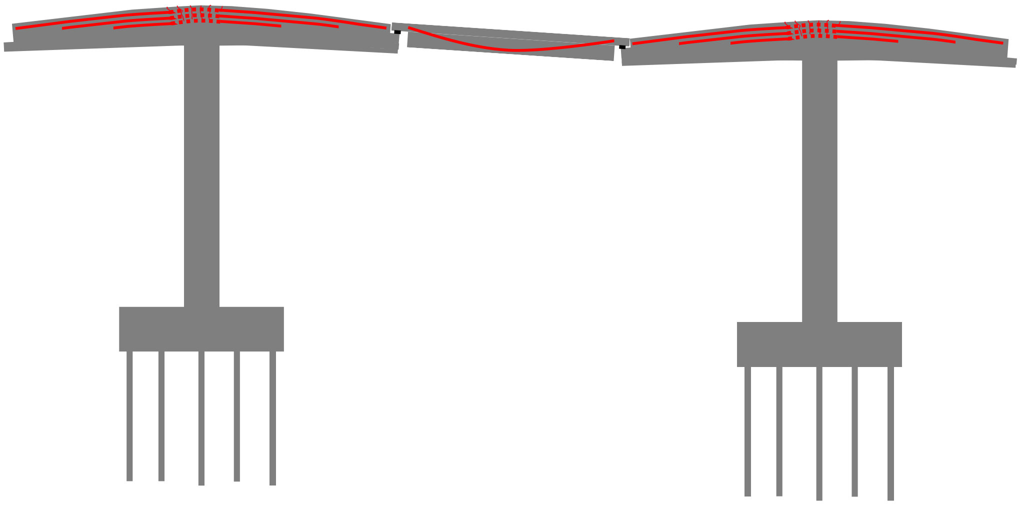

Figure 4: Current deteriorated condition of the cantilevers of the bridge after 48 years of service. The sketch shows the corrosion of the tendons above the piers (hypothesis based on extensive cracking observed on the locations) and the deflection of the deck (measured on a point cloud).

## 2.1 Geometry and materials

The part of the bridge under interrogation consists of 3 segmentally constructed balanced cantilever sets, extending 30 meters either side of the abutments. Neighboring cantilevers are connected by 40m long precast members forming an overall span of 100m. The geometry and individual sizes of the segments were measured in the original drawings and verified on a point cloud model. The position and trajectory of the prestressing tendons was not mentioned in the drawings so they were modelled according to standard practice of balance cantilever construction (all tendons on top flange of segment). Figure 5 depicts some critical cross sections of the cantilevers and details.

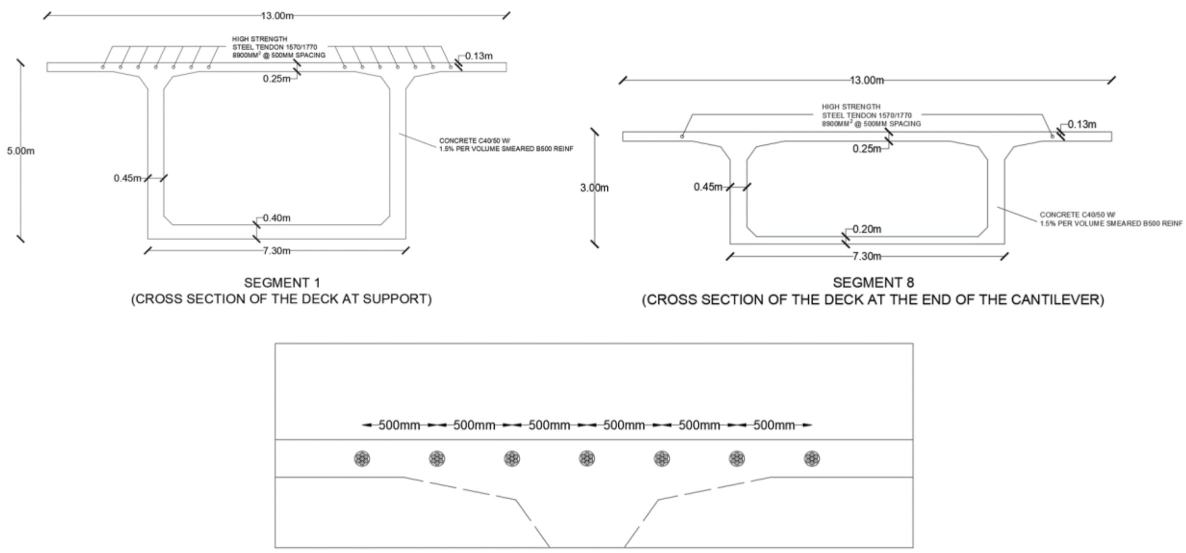


Figure 5: critical cross sections of the cantilevers and details.

Table 1: materials' properties.

| Material | Assumed properties |
|---|---|
| Reinforced concrete B450 | Young's modulus E= Varies<br>Compressive strength $f_{ck}$= 40 MPa<br>Tensile strength $f_{ctm}$ = 3.5 MPa<br>Ultimate strain $\varepsilon_{cu1}$= 3.5 ‰ |
| Prestressing steel 160/180 | Young's modulus E = 195 GPa<br>Tensile strength $f_{pk}$ = 1770 MPa<br>0.1% proof stress $f_{p0.1k}$ = 1570 |
| Passive reinforcement | Yield strength $f_{yk}$ = 500 MPa<br>Strain at maximum force $\varepsilon_{uk}$ = 2.5% |

The materials characteristics were found in the original design report, however their characteristic properties do not exactly match contemporary materials so a theoretical match was made between older and recent (Table 1). However, the fact that construction practice has come a long way since 1974 in terms of quality control, monitoring and protection against environmental parameters adds a degree of uncertainty. There is a number of mechanical properties that may have been affected by poor quality control:

- Young's modulus (E) and compressive strength of the in-situ cast concrete ($f_{ck}$)

- Strength of passive ($f_{yk}$) and active ($f_{pk}$) reinforcement
- Permeability of concrete, water/cement ratio (affecting the microscopic properties)
- Imperfections during casting leading to permanent displacements

### 2.2 Analysis and degradation assessment

The bridge was constructed as a hybrid of two methods, the majority of spans were simple cast in-situ concrete decks and the rest of them, which will be the focus of our investigation, were constructed as balanced cantilevers. To the best of the author's knowledge the damage mechanism hasn't been described accurately to this day, however expert judgment and literature suggest some probable reasons behind the faults. Although it is highly probable that a multitude of mechanisms are at work, a previous study [25] bypassed the underlying cause and focuses more on the damage manifestation, which has been assumed to be extensive corrosion within the prestressed tendons of the bridge deck. A thorough review of the existing drawings and expert judgement to cover for the missing information resulted in the preparation of a numerical model which was used to carry-out a predetermined amount of analyses based on an optimal input for the k-NN algorithm. The non-linear analyses included vertical loads and prestressing. All the results were then collected and used as an input to the prediction algorithm after undergoing some statistical processing. The quantitative of corrosion is estimated almost 50% based on back analyses of the balanced cantilevers [25].

The model used in the analysis was created in such a way that the analysis process would resemble the actual construction process (staged construction approach). Balanced cantilever segmental construction is an iterative process including a casting concrete stage followed directly by a prestressing stage after the concrete has reached the desired strength. So, in an endeavour to make the model follow the same principles the following reasoning was used; finite element analysis primarily revolves around stiffness, external forces and displacements in order to calculate the rest of the values like stress, strain etc. By significantly reducing the bending stiffness and by removing the self-weight of a segment it is made practically "undetectable" during the analysis. This property was used for the concrete elements, as it is not possible to create them with different timing through the analysis, contrary to the steel elements which can be inserted during a specific construction stage. To explain it in more detail, the modelling process is laid out below:

- Concrete elements have been defined with 35 GPa modulus of elasticity and 25 kN/m$^3$ self-weight.
- All concrete elements have been presented at the start of the analysis, however this contradicts the segmental construction process.
- The desired state is for the two central segments to be the only ones present at the beginning and all the others to be neglected in the calculations.
- By reducing the bending stiffness of segments 2-8 to almost zero and by not applying self-weight, their contribution to the overall stiffness and loading of the analysis is diminished.
- With each next construction stage, the properties of the next segment in line to be constructed will change and it will be able to bear loading and deflect together with the rest of the already casted concrete segments.

This change in properties can be induced by changing the material of the segments. In the beginning, a "soft" material is created and assigned to all segments except the first two (Construction stage 1). During the next part of the analysis, the first two segments are post-tensioned by tendons which are created with specific timing and the application of a tensile strain (construction stage 2). After post-tensioning the first two segments, the next set is casted; meaning that the Young's modulus and the self-weight of the concrete get their correct value (construction stage 3). An iterative process, alternating concrete casting and post-tensioning, is then followed until all 16 segments are completed (Table 2). At this point the only load on the girder is the self-weight of the prestressed segments, so the rest of the external loads are applied. A pre-cast girder, represented by a load of 7200 kN on each side, is applied on the deck followed by an area load considering the asphalt layers, sidewalks etc. evaluated at a uniform value of 2 kN/m$^2$ (Figure 20)

Table 2. Construction stages and their corresponding load cases (CC-concrete casting, PT-post tensioning).

| Construction stage # | Load case | Construction stage # | Load case |
|---|---|---|---|
| 1 | Segment 1 CC | 10 | Segment 5 PT |
| 2 | Segment 1 PT | 11 | Segment 6 CC |
| 3 | Segment 2 CC | 12 | Segment 6 PT |
| 4 | Segment 2 PT | 13 | Segment 7 CC |
| 5 | Segment 3 CC | 14 | Segment 7 PT |
| 6 | Segment 3 PT | 15 | Segment 8 CC |
| 7 | Segment 4 CC | 16 | Precast girder load |
| 8 | Segment 4 PT | 17 | Surface load |
| 9 | Segment 5 CC | | |

## 3 EXISTING DATA ON THE CURRENT CONDITION OF THE BRIDGE

The point cloud of the bridge with some details of the cantilever and the half-joint is depicted in Figure 6. The deflection of the most critical cantilever of the bridge is reported in Figure 7, where the dashed line is the expected elevation, while the solid line is the measured position, i.e. 133mm and 207mm lower than the expected. Such deflections are the cantilever displacements downward at the tip (end) of the most critical cantilever.

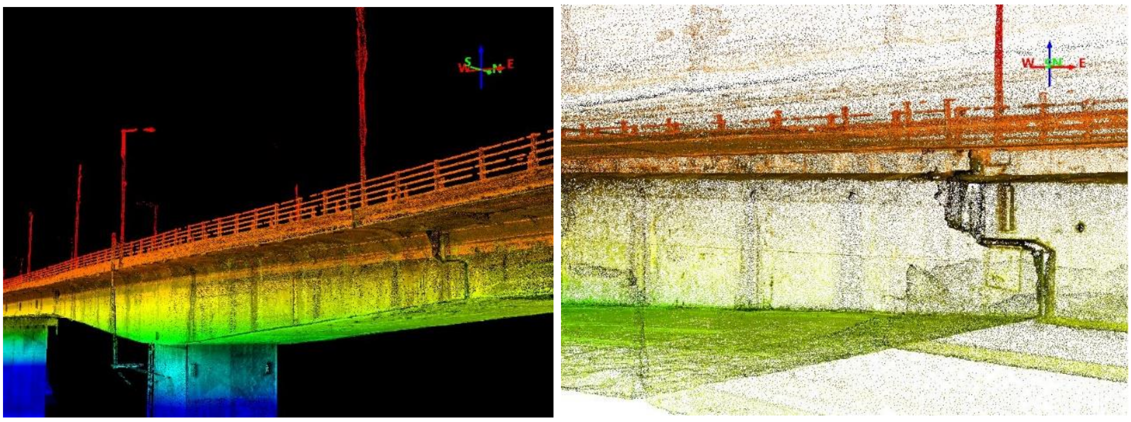

Figure 6: point cloud.

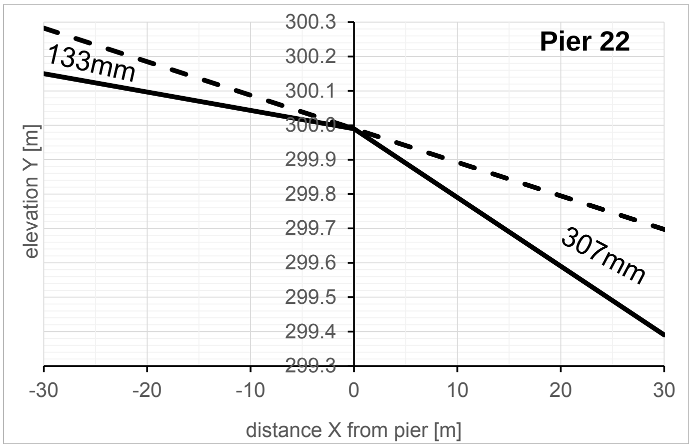


Figure 7: Measured deflection of the critical cantilever. Dashed line shows the hypothetical original elevation. Solid lines show the measured deflected cantilevers.

## 4 ADOPTED RETROFIT TECHNIQUES AND COST ASSESSMENT

In this section, the retrofitting techniques were preliminarily designed aiming to improve the structural performance of the bridge and enhance the safety levels by respecting standard regulation. As previously described, critical damages of the bridge can be manly attributed to insufficient maintenance strategies, possible poor workmanship at the construction phase, critical increase in the traffic levels and/or maximum traffic loads during the service-life and the aggressive environment. Critical losses of prestressing stress at the level of cantilever supports is the main cause of the functionality reduction as shown by Figure 4 and 7. For these reasons, two scenarios have been considered as feasible retrofitting solutions to restore the original serviceability of the bridge:

1. **Demolition and reconstruction:** this approach consists of demolishing the continuous deck composed by n.6 tapered box girder cantilevers and n.3 girder bridges, while existing piers have been maintained. It has been assumed that the reconstruction phase considers to maintain the same static scheme, materials and structural behaviors. This assumption can be considered reasonable since the bridge topology adopted by the designer is still widely used nowadays.
2. **Local interventions and replacement of the girder** bridge (Gerber bridge sections): in this scenario, external prestressing cables have been installed to restore the correct level of compression stresses into the n.6 cantilevers and the functionality of

the entire bridge. Moreover, the substitution of the n.3 girder bridge has been considered with a steel box girder section to avoid the corrosion effects into the prestressing cables. Therefore, as demonstrated by evaluations provided by the authors, this proposed solution results in an improvement of slenderness and an overall reduction of weight carried by cantilevers.

Once the retrofitting techniques have been identified, the authors proceed in order to define a detailed list of interventions for each scenario.
For scenario #1, the following activities have been considered:

a) Demolition of both defected balanced cantilever part of the deck and reinforced concrete girder bridge by adopting non-explosive agents with chemical action instead of explosive charges;
b) Reconstruction of decks by restoring the original static scheme of the bridge. In this phase, the authors have computed the cost for the construction for both concrete deck and steel reinforcement. The latter includes the steel reinforcement into the deck and the anchorages to fix the new cantilever to the existing piers' head;
c) Installation of elastomeric bearings at the end of the cantilever;
d) Installation of expansion joints at the level of the girder bridge deck in order to avoid thermal constraints or damage along the traffic pavement;
e) Road pavement realized by surfacing course top layer, asphalt bond coat, protective course, epoxy bonding layer, waterproofing and reinforced concrete deck;
f) Realization of all functional facilities like road signs, safety barriers, etc.

On the other hand, for scenario #2 the following activities have been taken into account:

a) Demolition of the Gerber bridge sections only adopting the same techniques of scenario 1;
b) Installation of a steel box deck which has been designed by adopting thumb rules aiming to reduce the total weight and assuring a minimum height for easier maintenance. Operations related to the realization of the reinforced concrete slab by adopting predalles system;
c) Application of hot-dip galvanizing (passivating treatment of the steel surface) to all steel surfaces of deck;
d) Substitution of girder deck bearings with FPS system aiming to avoid slip phenomena between deck and supports;
e) Installation of expansion joints at the level of the girder bridge deck in order to avoid thermal effect or damage along the traffic pavement;
f) Road pavement realized by surfacing course top layer, asphalt bond coat, protective course, epoxy bonding layer, waterproofing and reinforced concrete deck;
g) Realization of all functional facilities like road signs, safety barriers, etc;
h) External prestressing system realized by the addition of 4 cables along each cantilever in order to restore the original deflection. At this design stage, additional cables are supposed to be of the same section of that one recognized in the technical drawings. Moreover, the level of compression stress introduced into the system should be designed aiming to avoid cracking as depicted in Figure 8.

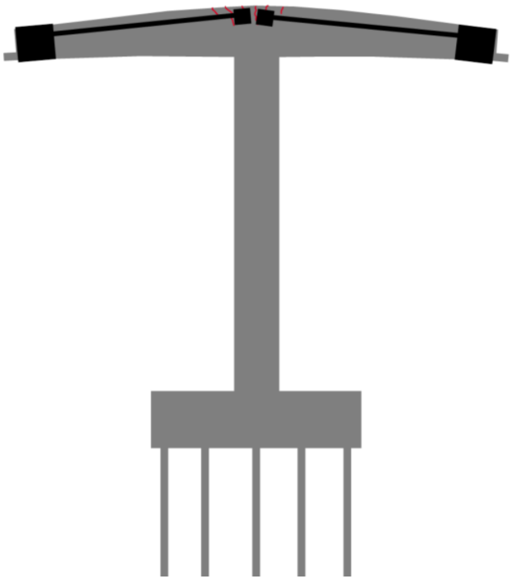

Figure 8: Scheme of prestressing system

The costs associated to each scenario have been evaluated by using the Italian price lists provided by ANAS S.p.A [26], with the exception of the prestressing system assessment for which the authors adopted the parametric cost pointed out by [27]. Thought price list may change from one country to another, although not drastically within the European community, authors focused mainly on the comparisons between different retrofitting scenarios.
Aiming to realize a comparison between the 2 scenarios, the authors selected a module of the bridge for which all the operations have been evaluated from an economical point of view (see Figure 9). The final amount of the estimations for each scenario is referred to the adopted module, hence, the cost of the overall intervention can be easily derived.

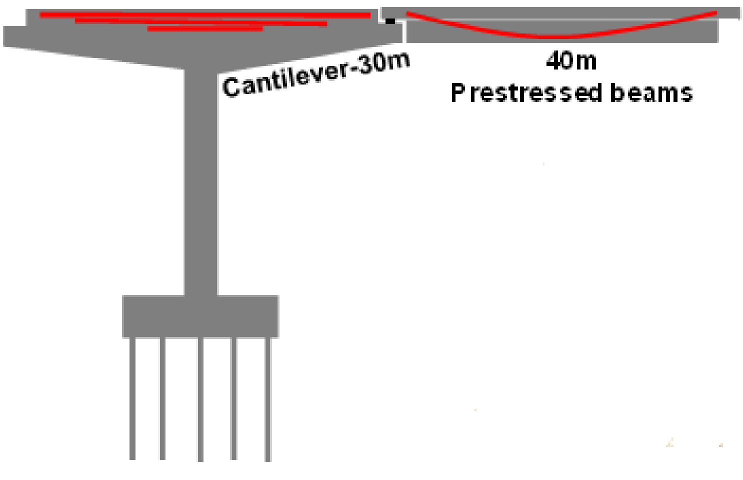


Figure 9: Module of the bridge considered for the cost evaluation

In Figures 10 and 11 report the spreadsheets with the calculations provided for each scenario. In the first column corresponds to the ID code of the adopted standard cost list. More details concerning with the description of the specific voice can be detected by ANAS S.p.A. [26]. The second column is a fast description of the activity. Columns 3 and 4 represent the unit for each operational phase and the geometrical properties of the considered element, respectively.

Finally, columns 5, 6 and 7 represent the total amount expressed in the unit indicated by the price list, the unit price and the total cost of the intervention, respectively.

| ID NUMBER | DESCRIPTION | U.M. | DIMENSIONS | | | | Amount | UNIT PRICE | TOTAL AMOUNT |
|---|---|---|---|---|---|---|---|---|---|
| | | | Numb. | L | P | H | | Euro | Euro |
| SCENARIO 1 | | | | | | | | | € 2.242.046,60 |
| A.03.008 | Bridge demolition phase | mc | - | - | - | - | 750,84 | € 107,43 | € 80.662,74 |
| B.08.025.b | Bridge constructon with precast segmental elements | mq | - | 100 | 13 | - | 1300 | € 1.423,39 | € 1.850.407,00 |
| B.07.070.a | Expantion joints | ml | 2 | - | 13 | - | 26 | € 522,05 | € 13.573,30 |
| Brdge supports | | | | | | | | | |
| B.07.007.a | uni-direction elastomeric bearings | kN | 6 | - | - | - | 3000 | € 3,74 | € 11.220,00 |
| Cast-in-place elements and reinforcement | | | | | | | | | |
| B.03.040.a | Slab concrete (Rck 40/50) | m^3 | - | 100 | 13 | 0,2 | 260 | € 203,64 | € 52.946,40 |
| B.05.050.a | Slab reinforcement | kg | - | - | - | - | 12940,2 | € 2,37 | € 30.668,27 |
| B.05.030 | Steel reinforcement (anchorages included) - B450C class | kg | - | - | - | - | 51695,28 | € 1,86 | € 96.153,22 |
| Pavement | | | | | | | | | |
| D.01.005.a | Primer layout (10 cm) | m^3 | - | 100 | 13 | 0,1 | 163,8 | € 162,68 | € 26.646,98 |
| B.06.085 | waterproofing layout (4 mm) | m^2 | - | 100 | 13 | 0,004 | 1300 | € 25,69 | € 33.397,00 |
| D.01.017.a | binder layout (10 cm) | m^3 | - | 100 | 13 | 0,1 | 163,8 | € 183,02 | € 29.978,68 |
| D.01.036.a | draining wear layer (4 mm) | m^2 | - | 100 | 13 | 0,004 | 1300 | € 12,61 | € 16.393,00 |
| FUNCTIONAL FACILITIES | | | | | | | | | € 1.820,00 |
| | Road signs | €/mq | - | 100 | 13 | - | 1300 | € 1,40 | € 1.820,00 |
| Electrical system | | | | | | | | | € 52.000,00 |
| | Electrical system | €/mq | - | 100 | 13 | - | 1300 | € 40,00 | € 52.000,00 |
| Drainage stormwater system | | | | | | | | | € 39.000,00 |
| | Drainage stormwater system | €/mq | - | 100 | 13 | - | 1300 | € 30,00 | € 39.000,00 |
| Safety barriers | | | | | | | | | € 40.789,00 |
| G.02.005.b | Safety barriers (class H4) | ml | - | 100 | - | - | 100 | € 407,89 | € 40.789,00 |
| | | | | | | | | Total | € 2.375.655,60 |

Figure 10. Detailed calculations provided for Scenario #1

| ID NUMBER | DESCRIPTION | U.M. | DIMENSIONS | | | | Amount | UNIT PRICE | TOTAL AMOUNT |
|---|---|---|---|---|---|---|---|---|---|
| | | | Numb. | L | P | H | | Euro | Euro |
| SCENARIO 2 | | | | | | | | | € 1.328.088,76 |
| A.03.008 | Bridge demolition phase | mc | - | - | - | - | 237,84 | € 107,43 | € 25.551,15 |
| B.05.008.b | Steel box bridge (incremental launching for lifting) | kg | - | 40 | 13 | | 194600 | € 5,61 | € 1.091.706,00 |
| B.09.160.a | Hot-dip galvanizing | m^2 | - | - | - | - | 520 | € 18,41 | € 9.573,20 |
| B.07.070.a | Expantion joints | ml | 2 | - | 13 | - | 26 | € 522,05 | € 13.573,30 |
| Brdge supports | | | | | | | | | |
| B.07.007.a | FPS isolation system bearings | kN | 6 | - | - | - | 3000 | € 3,74 | € 11.220,00 |
| Cast-in-place elements and reinforcement | | | | | | | | | |
| B.03.040.a | Slab concrete (Rck 40/50) | m^3 | - | 40 | 13 | 0,2 | 104 | € 203,64 | € 21.178,56 |
| B.05.050.a | Slab reinforcement | kg | - | - | - | - | 12940,2 | € 2,37 | € 30.668,27 |
| B.05.030 | Steel reinforcement (anchorages included) - B450C class | kg | - | - | - | - | 25847,64 | € 1,86 | € 48.076,61 |
| Pavement | | | | | | | | | |
| D.01.005.a | Primer layout (10 cm) | m^3 | - | 40 | 13 | 0,1 | 163,8 | € 162,68 | € 26.646,98 |
| B.06.085 | waterproofing layout (4 mm) | m^2 | - | 40 | 13 | 0,004 | 520 | € 25,69 | € 13.358,80 |
| D.01.017.a | binder layout (10 cm) | m^3 | - | 40 | 13 | 0,1 | 163,8 | € 183,02 | € 29.978,68 |
| D.01.036.a | draining wear layer (4 mm) | m^2 | - | 40 | 13 | 0,004 | 520 | € 12,61 | € 6.557,20 |
| FUNCTIONAL FACILITIES | | | | | | | | | € 728,00 |
| | Road signs | €/mq | - | 40 | 13 | - | 520 | € 1,40 | € 728,00 |
| Electrical system | | | | | | | | | € 20.800,00 |
| | Electrical system | €/mq | - | 40 | 13 | - | 520 | € 40,00 | € 20.800,00 |
| Drainage stormwater system | | | | | | | | | € 15.600,00 |
| | Drainage stormwater system | €/mq | - | 40 | 13 | - | 520 | € 30,00 | € 15.600,00 |
| Prestressing system | | | | | | | | | € 35.120,00 |
| AICAP | Prestressing system | ml | - | 40 | - | - | 40 | € 878,00 | € 35.120,00 |
| Safety barriers | | | | | | | | | € 16.315,60 |
| G.02.005.b | Safety barriers (class H4) | ml | - | 40 | - | - | 40 | € 407,89 | € 16.315,60 |
| | | | | | | | | Total | € 1.416.652,36 |

figure 11. Detailed calculations provided for Scenario #2

In table 3 and 4, each intervention has been collected in order to evaluate the total cost of each. The final value for each scenario has been expressed in terms of economical cost per km of bridge.

Table 3. Total interventions cost related to Scenario #1

| Activity | Cost (€) |
|---|---|
| (a) | 80.662,74 |
| (b) | 2.030.174,89 |
| (c) | 11.220,00 |
| (d) | 13.573,30 |
| (e) | 106.415,66 |

| | |
|---|---|
| (f) | 133.609,00 |
| **Total cost/km** | 1.827.427,38 |

Table 4. Total interventions cost related to Scenario #2

| Activity | Cost (€) |
|---|---|
| (a) | 25.551,15 |
| (b) | 1.191.629,44 |
| (c) | 9.573,00 |
| (d) | 11.200,00 |
| (e) | 13.573,30 |
| (f) | 76.541,66 |
| (g) | 53.443,60 |
| (h) | 35.120,00 |
| **Total cost/km** | 1.089.732,58 |

## 5 ENVIRONMENTAL IMPACT OF THE RETROFIT INTERVENTIONS

For the environmental sustainability assessment of the presented restoration scenarios, a Life Cycle Assessment (LCA) has been carried out according to ISO 14040 and ISO 14044 [28]. For LCA specifications regarding building products and construction works, European standards EN 15804, EN 15978 and EN15678 [29-3] have been furthermore considered.

As for the cost analysis, main goal of LCA is allowing a comparison between the different two scenarios and understanding their environmental impact on the whole infrastructure level, i.e. the bridge. Consequently, the established functional unit is the bridge surface ($km^2$ bridge). The analysis here presented is limited to the Global Warming Potential impact category (GWP 100ys, CML 2001), where the environmental data are provided from GENERIS® software [32] and selected from available product-specific (Environmental Product Declarations, EPD) and average generic construction materials' datasets [33]. Average datasets served also as a basis for a preliminary environmental assessment of products for which environmental information is not available, such as expansion joints, and bridge support systems. In particular, both bearing systems have been modelled as a double steel plate and an elastomeric intermediate element. Differently from cost analysis, in LCA functional facilities, electrical systems, drainage stormwater system and safety barriers are neglected. These are in fact deemed out of scope of the analysis, which is focused rather on the restoration scenarios solely.

Figures 12 and 13 outline the data collected for the Lifecycle Inventory (LCI) and the subsequent Lifecycle Impact Assessment (LCIA) stage. Each material is matched with a suitable environmental dataset. For a correct dataset match, products' composition, densities and applications are checked. Afterwards, lifecycle information regarding GWP is extracted. The environmental impact is calculated for the total products' amount and, lastly, the environmental impact of the scenario is derived per $km^2$ bridge.

| ID NUMBER | DESCRIPTION | Selected dataset | Dataset type | Lifecycle phases [EN15978] | Density [kg/m³] | Reference Unit | GWP [kg CO2 eq./unit] | Amount | Total |
|---|---|---|---|---|---|---|---|---|---|
| **SCENARIO 1** | | | | | | | | | |
| A.03.008 | Bridge demolition phase | Spannbeton-Fertigteildecken | EPD | C3-C4; D | | m³ | *228.92* | 751 | 171885.7 |
| B.08.025.b | Bridge construction with precast segmental elements | Spannbeton-Fertigteildecken | EPD | A1-A3; C3-C4; D | | m² | *58.19* | 1300 | 75644.4 |
| B.07.070.a | Expantion joints | Bitumen-based adhesive(60% Bitumen, 23%LM, 17% Water) | avarage | A1-A3; C3-C4; D | *930* | kg | *0.61* | 628680 | 385569.4 |
| **Bridge supports** | | | | | | | | | |
| B.07.007.a | uni-direction elastomeric bearings | Steel sections + Elastomer | avarage | A1-A3; C3-C4; D | | item | *10.18* | 3000 | 30546.8 |
| **Cast-in-place elements and reinforcement** | | | | | | | | | |
| B.03.040.a | Slab concrete (Rck 40/50) | Beton der Druckfestigkeitsklasse C 45/55 | EPD | A1-A3; C3-C4; D | *2400* | | *270.61* | 260 | 70358.6 |
| B.05.050.a | Slab reinforcement | Reinforcement steel | avarage | A1-A3; C3-C4; D | *7850* | kg | *0.29* | 12940 | 3766.7 |
| B.05.030 | Steel reinforcement (anchorages included) - B450C class | Reinforcement steel | avarage | A1-A3; C3-C4; D | *7850* | kg | *0.29* | 51695 | 15047.6 |
| **Pavement** | | | | | | | | | |
| D.01.005.a | Primer layout (10 cm) | Bitumen-based adhesive(60% Bitumen, 23%LM, 17% Water) | avarage | A1-A3; C3-C4; D | *1300* | kg | *0.6133* | 212940 | 130596.1 |
| B.06.085 | waterproofing layout (4 mm) | Joint sealing strips, polyisobutylene | avarage | A1-A3; C3-C4; D | *1300* | kg | *5.821* | 6760 | 39350.0 |
| D.01.017.a | binder layout (10 cm) | Binder Products based on epoxy-resin | EPD | A1-A3; C3-C4; D | *1750* | kg | *11.1756* | 286650 | 3203485.7 |
| D.01.036.a | draining wear layer (4 mm) | Bitumen emulsion (40% bitumen, 60% water) | avarage | A1-A3; C3-C4; D | *1000* | kg | *0.41524* | 5200 | 2159.2 |
| **FUNCTIONAL FACILITIES** | | | | | | | | | |
| **Electrical system** | | | | | | | | | |
| **Drainage stormwater system** | | | | | | | | | |
| **Safety barriers** | | | | | | | | | |
| | | | | | | | | | |
| | | | | | | | **Total GWP [kg CO2eq.]** | | **4128410.26** |
| | | | | | | | **GWP [kg CO2eq./km²]** | | **3175700.20** |

Figure 12: LCA, Scenario 1. Lifecycle impact assessment.

| ID NUMBER | DESCRIPTION | Selected dataset | Dataset type | Lifecycle phases [EN15978] | Density [kg/m³] | Reference Unit | GWP [kg CO2 eq./unit] | Amount | Total |
|---|---|---|---|---|---|---|---|---|---|
| **SCENARIO 2** | | | | | | | | | |
| A.03.008 | Bridge demolition phase | Spannbeton-Fertigteildecken | EPD | C3-C4; D | | m³ | *228.925* | 238 | 54447.41 |
| B.05.008.b | Steel box bridge (incremental launching for lifting) | Steel sections | avarage | A1-A3; C3-C4; D | *7850* | kg | *0.7714* | 194600 | 150114.44 |
| B.09.160.a | Hot-dip galvanizing | Hot dip galvanized steel; area weight | avarage | A1-A3; C3-C4; D | *7850* | m² | *7.394* | 520 | 3844.88 |
| B.07.070.a | Expantion joints | Bitumem based adhesive | avarage | A1-A3; C3-C4; D | *930* | kg | *0.6133* | 628680 | 385569.44 |
| **Bridge supports** | | | | | | | | | |
| B.07.007.a | FPS isolation system bearings | Steel sections + Elastomer | avarage | A1-A3; C3-C4; D | | item | *10.1822821* | 3000 | 30546.85 |
| **Cast-in-place elements and reinforcement** | | | | | | | | | |
| B.03.040.a | Slab concrete (Rck 40/50) | Beton der Druckfestigkeitsklasse C 45/55 | EPD | A1-A3; C3-C4; D | *2400* | m³ | *270.61* | 104 | 28143.44 |
| B.05.050.a | Slab reinforcement | Reinforcement steel | avarage | A1-A3; C3-C4; D | *7850* | kg | *0.2910821* | 12940 | 3766.66 |
| B.05.030 | Steel reinforcement (anchorages included) - B450C class | Reinforcement steel | avarage | A1-A3; C3-C4; D | *7850* | kg | *0.2910821* | 25848 | 7523.79 |
| **Pavement** | | | | | | | | | |
| D.01.005.a | Primer layout (10 cm) | Bitumen-based adhesive (60% Bitumen, 23%LM, 17% Wasser) | avarage | A1-A3; C3-C4; D | *1300* | kg | *0.6133* | 212940 | 130596.10 |
| B.06.085 | waterproofing layout (4 mm) | Joint sealing strips, polyisobutylene | EPD | A1-A3; C3-C4; D | *1300* | kg | *5.821* | 2704 | 15739.98 |
| D.01.017.a | binder layout (10 cm) | Binder Products based on epoxy-resin | EPD | A1-A3; C3-C4; D | *1750* | kg | *11.1756* | 286650 | 3203485.74 |
| D.01.036.a | draining wear layer (4 mm) | Bitumen emulsion (40% bitumen, 60% water); | avarage | A1-A3; C3-C4; D | *1000* | kg | *0.41524* | 2080 | 863.70 |
| **FUNCTIONAL FACILITIES** | out of scope; neglected | | | | | | | | |
| **Electrical system** | | | | | | | | | |
| **Drainage stormwater system** | | | | | | | | | |
| **Prestressing system** | | | | | | | | | |
| **Safety barriers** | | | | | | | | | |
| | | | | | | | **Total GWP [kg CO2eq.]** | | **4014642.43** |
| | | | | | | | **GWP [kg CO2eq./km²]** | | **3088186.49** |

Figure 13: LCA, Scenario 1. Lifecycle impact assessment.

Analogously with cost analysis, in table 5 and 6, GWP is calculated and aggregated in interventions.

Table 5. Total interventions GWP related to Scenario #1

| Activity | GWP [kg CO2eq] |
|---|---|
| (a) | 171 885.69 |
| (b) | 164 817.23 |
| (c) | 30 546.85 |
| (d) | 385 569.44 |

| | |
|---|---|
| (e) | 3 373 431.80 |
| (f) | out of scope |
| **Total GWP** | **4 126 251.02** |
| **Total GWP /km²** | **3 174 039.24** |

Table 6. Total interventions GWP related to Scenario #2

| Activity | GWP [kg CO2eq] |
|---|---|
| (a) | 54 447.41 |
| (b) | 189 548.33 |
| (c) | 38 44.88 |
| (d) | 30 546.85 |
| (e) | 385 569.44 |
| (f) | 3 350 685.53 |
| (g) | out of scope |
| (h) | out of scope |
| (i) | out of scope |
| **Total GWP** | **4 014 642.43** |
| **Total GWP /km²** | **3 088 186.49** |

## 6 CONCLUSIONS

- This preliminary study arises from the need to evaluate possible retrofit interventions for the degradation of the Polyfytos bridge.
- Different interventions have been evaluated with respect to costs and their environments sustenaibility.
- The study is based on state-of-the-art surveying tools (laser-photogrammetry) paired with an advanced analysis to the Polyfytos bridge.
- The preliminary results show a reasonable equivalence in terms of environmental sustainability with an essential difference in terms of costs of intervention.
- Although the study is preliminary with a limited number of scenarios, it is observed that there is a difference between the two types of intervention in terms of cost that was expected. Forthcoming developments intend to consider additional scenarios and parameters for evaluating the possible interventions, such as the validity of each solution over time.

**ACKNOWLEDGMENT**

The research leading to these results has received funding from the European Research 501 Council under the Grant agreement ID: 101007595 of the project ADDOPTML, MSCA RISE 502 2020 Marie Skodowska Curie Research and Innovation Staff Exchange (RISE). Paola Cavallaro is gratefully acknowledgement for supporting LCA preliminary analysis.

## REFERENCES


[1] Concrete Bridge Development Group, *Development of prestressed concrete bridges*, 2017. https://www.cbdg.org.uk/

[2] Z.P. Bažant, J.C. Chern Bayesian statistical prediction of concrete creep and shrinkage, *ACI Journal*, **81** (4), 319-330, 1984.

[3] Z.P. Bažant, J.K. Kim Improved prediction model for time-dependent deformations of concrete: Part 2 - basic creep, *Mater. Struct.*, **24** (6), 1991.

[4] Z.P. Bažant, L. Panula Creep Shrinkage Characterization for Prestressed Concrete Structures, *J. of the Prestressed Concrete Institute*, **25**, 86-122, 1980.

[5] N. Lu, M. Beer, M. Noori, Y. Liu Lifetime Deflections of Long-Span Bridges under Dynamic and Growing Traffic Loads, *J. Bridge Eng.*, 04017086, 1-12, 2017

[6] M. Morgese, F. Ansari, M. Domaneschi, G. P. Cimellaro, Post-collapse analysis of Morandi's Polcevera viaduct in Genoa Italy, *Journal of Civil Structural Health Monitoring*, **10**, 69–85, 2020.

[7] G. Lucko, Jesu´s M. de la Garza, Constructability Considerations for Balanced Cantilever Construction, *Pract. Period. Struct. Des. Constr*., **8**(1): 47-56, 2003.

[8] T. Guo, R. Sause, D. Frangopol, A. Li, Time-Dependent Reliability of PSC Box-Girder Bridge Considering Creep, Shrinkage, and Corrosion, *J. Bridge Eng*., **16**(1): 29-43, 2011.

[9] S. Wang, C.C. Fu, Simplification of Creep and Shrinkage Analysis of Segmental Bridges, *J. Bridge Eng*., **20**(8): B6014001, 2015.

[10] M. Domaneschi, C. Pellecchia, E. De Iuliis, G. P. Cimellaro, M. Morgese, A.A. Khalil, F. Ansari, Collapse analysis of the Polcevera Viaduct by the Applied Element Method", *Engineering Structures*, **214**, 110659, 2020.

[11] S. Varbla, E.Artu, P. Raido, Centimetre-range deformations of built environment revealed by drone-based photogrammetry, *Automation in Construction*, **128**, 103787, 2021.

[12] Lõhmus, H., et al. "Terrestrial laser scanning for the monitoring of bridge load tests–two case studies." Survey review 50.360 (2018): 270-284.

[13] T.R. Witcher, From disaster to prevention: The silver bridge, *Civil Engineering Magazine Archive*, **87**(11), 44-47, 2017.

[14] Z.P. Bažant, Q. Yu, G.H. Li, Excessive long-time deflections of prestressed box girders. I: Record-span bridge in Palau and other paradigms, *Journal of structural engineering* **138**(6), 676-686, 2012.

[15] SGS https://www.sgs.com/en

[16] O. Markogiannaki, X. Hang, F. Chen, S. Mitoulis, I. Parcharidis Monitoring of a landmark bridge using SAR interferometry coupled with engineering data and forensics, *International Journal of Remote Sensing*, **43**, 95-119, 2022.

[17] S. Li, W. Wang, B. Lu, X. Du, M. Dong, T. Zhang, Z. Bai Long-term structural health monitoring for bridge based on back propagation neural network and long and short-term memory, *Structural Health Monitoring*, 14759217221122337, 2022.

[18] J. Zhou, Z. Sun, B. Wei, L. Zhang, P. Zeng, P., Deflection-based multilevel structural condition assessment of long-span prestressed concrete girder bridges using a connected pipe system, *Measurement*, 169, 108352, 2021.

[19] Bažant 2015

[20] Bažant 2018

[21] Strauss 2017

[22] Lee 2019

[23] W. Podolny Corrosion of prestressing steels and its mitigation, *PCI journal* **37**(5), 34-55, 1992.

[24] W.H. Hartt, S. Venugopalan *Corrosion evaluation of post-tensioned tendons on the Mid Bay Bridge in Destin*, Florida, Florida Department of Transportation Research Center report 33890, 2002.

[25] Ref for the k-NN analyses and estimation of 50% corrosion in prestressing strands

[26] ANAS S.p.A. (2022), Price list for New Construction and scheduled maintenance (in Italian). https://www.stradeanas.it/it/elenco-prezzi

[27] A. Devitofranceschi Repair of prestressed road viaducts: intervention techniques and cost-benefit analysis (in Italian) *Italian Concrete Days-AICAP*, 2018.

[28] International Organization for Standardization 2006 Principles and Framework (Geneva, Switzerland) Environmental management- Life cycle assessment ISO EN 14040:2006

[29] International Organization for Standardization 2006 Environmental management- Life cycle assessment - Requirements and guidelines (Geneva, Switzerland) ISO EN 14044:2006

[30] European Committee for Standardization 2020 Sustainability of construction works - Environmental product declarations - Core rules for the product category of construction products (Brussels, Belgium) EN 15804:2020 https://www.cencenelec.eu

[31] European Committee for Standardization 2011 Calculation method (Brussels, Belgium) Sustainability of construction works. Assessment of environmental performance of buildings EN 15978:2011 https://www.cencenelec.eu

[32] Fraunhofer IBP GENERIS®: www.generis-solution.eu

[33] Im BBSR Ö D ÖKOBAUDAT https://oekobaudat.de/